Journal of Atmospheric and Terrestrial Physics, Vol. 50, Nos 4/5, pp. 423–446, 1988.
Printed in Great Britain.

0021–9169/88 $3.00+ .00
Pergamon Press plc

Flow in the high latitude ionosphere: measurements at 15 s resolution made using the EISCAT 'Polar' experiment

H. TODD, S. W. H. COWLEY, A. ETEMADI
Blackett Laboratory, Imperial College, London SW7 2BZ, U.K.

B. J. I. BROMAGE, M. LOCKWOOD, D. M. WILLIS
Rutherford Appleton Laboratory, Chilton, Didcot, Oxon OX11 0QX, U.K.

and

H. LÜHR
Institut fur Geophysik und Meteorologie der Technischen Universität Carolo-Wilhelmina, 3300 Braunschweig, F.R.G.

Abstract—We present a first overview of flows in the high latitude ionosphere observed at 15 s resolution using the U.K.-Polar EISCAT experiment. Data are described from experiments conducted on two days, 27 October 1984 and 29 August 1985, which together span the local times between about 0200 and 2130 MLT and cover five different regions of ionospheric flow. With increasing local time, these are: the dawn auroral zone flow cell, the dayside region of low background flows equatorward of the flow cells, the dusk auroral zone flow cell, the boundary region between the dusk auroral zone and the polar cap, and the evening polar cap. Flows in both the equatorward and poleward portions of the auroral zone cells appear to be relatively smooth, while in the central region of high speed flow considerable variations are generally present. These have the form of irregular fluctuations on a wide range of time scales in the early morning dawn cell, and impulsive wave-like variations with periods of a few minutes in the afternoon dusk cell. In the dayside region between the flow cells, the ionosphere is often essentially stagnant for long intervals, but low amplitude ULF waves with a period of about 5 min can also occur and persist for many cycles. These conditions are punctuated at one to two hour intervals by sudden 'flow burst' events with impulsively generated damped wave trains. Initial burst flows are generally directed poleward and can peak at line-of-sight speeds in excess of 1 km s^{-1} after perhaps 45 s. Flows in the polar cap are reasonably smooth on time scales of a few minutes and show no evidence for the presence of ULF waves. Under most, but not all, of the above conditions, the beam-swinging algorithm used to determine background vector flows should produce meaningful results. Comparison of these flow data with simultaneous plasma and magnetic field measurements in the solar wind, made by the AMPTE IRM and UKS spacecraft, emphasizes the strong control exerted on high latitude flows by the north–south component of the IMF.

1. INTRODUCTION

Incoherent scatter radars have been used over the past fifteen years to measure the plasma flows which occur in the auroral zone ionosphere. Flow experiments run on monostatic (single transmitter receiver) systems, such as those at Chatanika, Millstone Hill and Sondrestromfjord, have employed beam-swinging techniques for this purpose, in which line-of-sight (l-o-s) speeds measured at a given latitude in two or more directions are combined to deduce the vector flow (DOUPNIK *et al.*, 1972; EVANS *et al.*, 1980; WICKWAR *et al.*, 1984). The radar dwells typically 1–5 min in each pointing direction, and the ionospheric scattering volumes from which a given flow vector is deduced are typically separated (in longitude) by a few hundred kilometres. In employing such techniques it is thus effectively assumed that the flow is steady over periods of several minutes, and uniform (in longitude) over distances of the order of a hundred kilometres.

When the radar is directed at low elevation angles, l-o-s speeds can usually be obtained simultaneously over a small range (a few degrees) of invariant latitude by gating the backscattered signal, but the range can be extended by making measurements at several different elevations. With dwell times at each position of a few minutes however, the experiment cycle times are thereby extended to a few tens of minutes. Most recent experiments have concentrated on investigating flows over a wide range of invariant latitudes using, for example, five or more separate elevation angles, with resulting cycle times of typically 15–30 min. These experiments have served to clarify the pattern of the large scale twin cell flow at high latitudes, and its dependence on geomagnetic activity and on the interplanetary magnetic field (IMF) direction (EVANS *et al.*, 1980; FOSTER *et al.*, 1981, 1982; FOSTER, 1983; OLIVER *et al.*, 1983; CLAUER *et al.*, 1984; JORGENSEN *et al.*, 1984; FOSTER and DOUPNIK, 1984; CLAUER and BANKS, 1986). More recently, large scale auroral zone flows have also been investigated using the tristatic EISCAT system, again using multi-point latitudinal scans having cycle times of about 30 min (ALCAYDÉ *et al.*, 1986; FONTAINE *et al.*, 1986).

It is important for several reasons, however, to investigate the flow at much higher temporal resolution than has been possible with these experiments. For example, it is known that the large scale ionospheric flow responds to changes in the IMF on time scales as short as a few minutes (RISHBETH *et al.*, 1985). In addition, high temporal resolution (and preferably high spatial resolution as well) is required to study the ionospheric counterparts of small scale magnetospheric phenomena whose importance has been widely recognized in recent years. A particularly important example is localized, transient reconnection at the dayside magnetopause which gives rise to flux transfer events (FTEs). These are expected to produce bursts of rapid flow in the ionosphere (a few km s^{-1}) near the dayside cusp. Since the horizontal scale of a FTE in the ionosphere is typically expected to be a few hundred kilometres, its duration at a given location will be just a few minutes (COWLEY, 1984, 1986; SOUTHWOOD, 1985, 1987; LEE, 1987). The transient flow pulsations which these and other perturbations excite on adjacent flux tubes at high latitudes have similar periods. Of course, coherent scatter radars such as STARE and SABRE (GREENWALD *et al.*, 1978; NIELSEN *et al.*, 1983), which can produce an array of vectors with a spatial resolution of 20 km every 20 s, are capable of resolving such structures, and evidence of their observation has recently been presented by NIELSEN (1984), SOFKO *et al.* (1985) and GOERTZ *et al.* (1985). These systems are, however, limited by threshold effects, uncertainties in the interpretation of the deduced flow speeds (ROBINSON, 1986; SCHLEGEL *et al.*, 1986) and their inability to determine ionospheric plasma parameters simultaneously. A more important limitation of existing systems with regard to FTE studies, however, is that they are located at latitudes where they encounter the auroral oval near noon (the cusp) only under conditions of extreme magnetic disturbance.

Auroral zone incoherent scatter radars do not suffer from these limitations, but, as explained above, the experiments employed to measure ionospheric flows have had cycle times which are, generally, more than an order of magnitude longer than is required to resolve the perturbations expected. In this paper we describe results obtained using the EISCAT UHF U.K. Special Programme experiment 'Polar', which was devised with the initial aim of determining the ionospheric vector flow in the vicinity of the dayside cusp with a temporal resolution of a few minutes (VAN EYKEN *et al.*, 1984; WILLIS *et al.*, 1986). Since the cusp is generally located far to the north of the EISCAT transmitter site at Tromsø (invariant latitude 66.3°), the EISCAT tristatic geometry is unfavourable and the experiment again uses beam-swinging to determine flow vectors. The standard 'Polar' experiment has a full cycle time of 5 min and the data are routinely analysed to produce a latitude profile of the vector flow every 2.5 min, as described further in the next section. These data have already been used in several studies of high latitude dayside flows and their dependence on the IMF (RISHBETH *et al.*, 1985; WILLIS *et al.*, 1986; ETEMADI *et al.*, 1988).

However, latitude profiles of the l-o-s velocity component are recorded every 15 s during these experiments, which equals the temporal, if not the spatial, resolution of coherent scatter radar systems. TODD *et al.* (1986) have used this 15 s data to describe the structure of a brief burst of flow observed in the dayside sector, which was suggested to be the ionospheric signature of a flux transfer event. During the same burst of rapid flow, LOCKWOOD *et al.* (1987) discovered evidence for the existence of non-Maxwellian ionospheric ion distribution functions, driven by ion–neutral collisions. The l-o-s flow data (post integrated to 30 s) have also been used by LOCKWOOD *et al.* (1986) to investigate a sudden post-noon onset of flow which followed a southward turning of the IMF. In these applications 'Polar' should be regarded as an experiment which primarily determines the scalar l-o-s speed over a restricted range of latitudes with very high time resolution, but where the beam direction is swung periodically in order to derive coarser information about the direction and strength of the large scale flow.

The purpose of this paper is to provide a first overview of the 15 s 'Polar' data. To do this we simply describe the main features of the flow observed at this resolution at different local times during two typical 'Polar' runs. The first of these experiments, to be described in Section 3, was conducted on 27 October 1984 and covered the local time interval between about 0200 and 1800 MLT. Particular features of the data obtained on that day have been discussed previously by RISHBETH *et al.* (1985), LOCKWOOD *et al.* (1986, 1987) and TODD *et al.* (1986), as mentioned above. This overview therefore helps to place these more restricted studies into context. Data from the

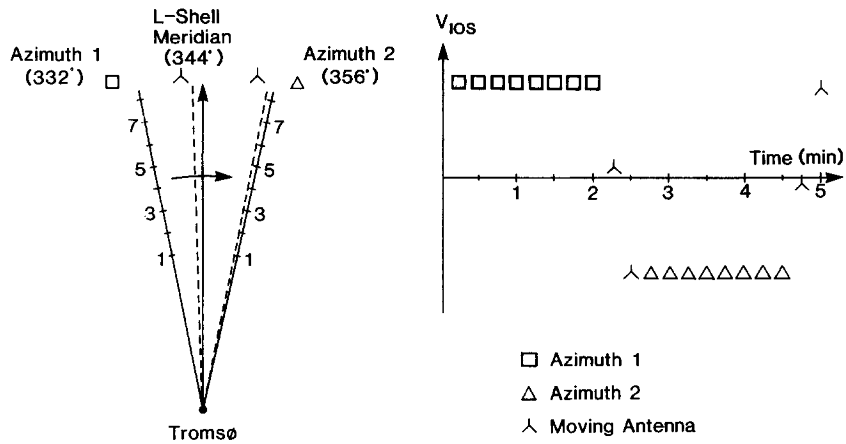

Fig. 1. (Left) Sketch of the geometry of the EISCAT 'Polar' experiment in a view looking down upon the ionosphere. The directions of the radar beams in the two dwell positions are shown by the solid lines marked 'azimuth 1' and 'azimuth 2', the angles given referring to geographic azimuths about the Tromsø transmitter site. The two directions are separated in azimuth by 24°, equally about the local L-shell meridian, and are pointed at a low elevation angle of 21.5°. The tick marks along these lines represent the centres of the 75 km long range gates employed, gate 1 being centred at a range of 525 km. The dashed lines show the mean azimuths of the two 15 s measurements made while the antenna was in motion between the dwell positions, for the case of the swing from azimuth 1 to azimuth 2, as indicated by the arrow. For the return swing the mean positions are the mirror images about the centre line. Also shown are the symbols used to plot the data from each position. (Right) Sketch of the form of the 15 s 'Polar' l-o-s velocity data. Eight consecutive 15 s measurements are made in each dwell position (squares for azimuth 1 and triangles for azimuth 2), followed by two 15 s measurements during which the antenna is in motion. The experiment cycle thus consists of 2 min dwell periods and two 30 s periods during which the antenna moves, with a total cycle time of 5 min. In this plot we have assumed for definiteness that the ionospheric flow is exactly westward directed, such that the l-o-s flows measured at the two 'Polar' azimuths are equal and opposite. Flows away from the radar are taken as positive.

second experiment, conducted on 29 August 1985 and described here in Section 4, cover the interval between about 1230 and 2130 MLT, and have not been described previously. It is found that basic features of the flow are similar on the two days, but that there are also differences, which appear to be related to the different character of the prevailing IMF conditions. We begin in the next section, however, by giving details of the 'Polar' experiment and the analysis of its data, and also introduce the format of the figures to be used in Sections 3 and 4.

2. THE POLAR EXPERIMENT AND FORMAT OF THE 15s DATA

In order to determine ionospheric flows as far to the north of the Tromsø transmitter site as possible, the 'Polar' radar beam is directed at a low elevation angle (21.5°, determined by the horizon profile) and is then swung successively between two northward-pointing azimuths. The geometrical arrangement is sketched in Fig. 1, together with the consequent format of the 15 s data. On the left hand side of the figure the directions of the two radar dwell positions are indicated by the solid lines, in a view from above the ionosphere. These are at geographic azimuths 332° and 356° (referred to below as azimuths 1 and 2, respectively), 12° on either side of the L shell meridian at Tromsø (344°). Equal ranges along the two beams therefore correspond to nearly equal invariant latitudes. The tick marks along the two beam directions indicate the centres of the range gates employed, which start at an invariant latitude of 70.8° and are separated by 0.6°. The corresponding heights start at 211 km with increments of 33 km. In this paper we present 15 s data from gates 1–4, corresponding to invariant latitudes from 70.8° to 72.6°, and heights from 211 to 311 km. The longitudinal separation of the two scattering volumes at a given invariant latitude increases from about 220 km at gate 1 to about 310 km at gate 4.

The 5 min cycle time of the standard 'Polar' experiment consists of a 2 min dwell at both azimuths 1 and 2, each being followed by a 30 s period during which the antenna moves. Data are integrated and recorded every 15 s throughout the cycle (including when the antenna is moving), so that 8 measurements are made during each dwell, followed by 2 measurements during which the antenna moves. The antenna actually takes only 23 s to move between the two dwell positions, so that most of the antenna displacement takes place in the first of these 'moving' measurements, whereas the antenna is at rest at the new dwell position for 7 s before the start of the next 'dwell' measurement. By taking account of the accelerations of the antenna, we estimate that the mean azimuth during the first of the 'moving' measurements is displaced from the old azimuth by nearly 10°, corresponding to a position nearly half way between the two dwell positions, whereas the mean azimuth for the second is within 1° of the new azimuth. These positions are indicated by the dashed lines in the sketch on the left hand side of Fig. 1 for the swing from azimuth 1 to azimuth 2. For the movement from azimuth 2 back to azimuth 1 the mean positions are the mirror images about the centre line.

On the right hand side of Fig. 1 we show schematically the format of the 15 s data which results from the 'Polar' experiment described above. This shows the l-o-s velocity component, V_{los}, vs. time for one gate during a complete experiment cycle (starting at the beginning of the azimuth 1 dwell), where we have assumed for definiteness that a steady, uniform westward flow is present across the field of view. Measurements at azimuths 1 and 2 are plotted as squares and triangles, respectively, while measurements made during antenna movements are shown by the inverted Y symbols. Here, and throughout the paper, we have adopted the convention that velocities away from the radar along the beam directions are positive. Consequently, for a pure westward flow we observe positive l-o-s components at azimuth 1 and negative l-o-s components of equal magnitude at azimuth 2. For pure eastward flows these signs would be reversed. The effect of introducing an additional north–south flow component is to displace the pattern from symmetry about the line $V_{los} = 0$ to net positive values for northward flows and net negative values for southward flows. A flow deflection of 12° from the east–west direction is required to reduce one of the l-o-s speeds to zero. It is easy, therefore, to determine the signs of the north–south and east–west components of the flow from visual inspection of this data. Of course, precise determination of the flow speed and direction requires detailed analysis of the dwell averaged beam-swinging data, taking account of the radar beam and magnetic field geometry, and velocities derived on this basis will be given below as appropriate. It should be noted that in this analysis, as well as in the discussion throughout the paper, it is assumed that the contribution of field-aligned components of the plasma flow to the observed l-o-s components is negligible. The 'Polar' experiment is insensitive to such flows because of the large angle of inclination between the radar beams and the F-region magnetic field within the field-of-view (73.5°). In any case, these flows are generally expected to be of much smaller magnitude than the $\mathbf{E} \times \mathbf{B}$ drifts. With this assumption a latitude profile of the vector flow transverse to the field can then be routinely derived from the dwell averaged data every 2.5 min, by combining the l-o-s velocity components measured during each dwell with a linearly interpolated value from the two adjacent dwells at the other azimuth (WILLIS et al., 1986). Vector flow maps derived on this basis are presented in the following sections in order to set the 15 s data into context.

In Fig. 2 we present simultaneous IMF and 'Polar' 15 s data in the format to be employed in the following sections. The lower four panels show half an hour of 'Polar' V_{los} data for gates 1–4 obtained between 1530 and 1600 UT on 29 August 1985, each gate being labelled by its invariant latitude. The extremes of the V_{los} scale of each panel correspond to ± 1 km s^{-1} and these values are used for all similar figures presented in this paper. We have purposefully chosen not to optimize the V_{los} scale for each plot in order that relative V_{los} values can be easily compared from figure to figure. The symbols and sign convention employed in Fig. 2 are identical to those discussed above in relation to the right hand side of Fig. 1, each symbol being plotted at the end of the 15 s interval to which it refers. Comparison of the form of the data with Fig. 1 immediately shows that the background flow is directed towards the north-west at the beginning of this interval, turning steadily westward towards its end. Since the magnetic local time (MLT) at the centre of the 'Polar' field-of-view is approximately 2.5 h later than UT, these data were obtained in the immediate post dusk hours from about 1800 to 1830 MLT. The generally westward (sunward) flows observed then clearly correspond to the early evening flows of the dusk auroral zone flow cell. The value of V_{los} for the first of the measurements made when the antenna was in motion (inverted Y symbols) generally lies roughly half way between adjacent 'dwell' values, while that for the second generally lies close to the values recorded during the subsequent dwell, in accordance with the discussion above concerning the mean directions in which these measurements were made.

Figure 2 illustrates how, for much of the time, the 'Polar' data exhibit excellent consistency, from point to point, gate to gate and dwell to dwell, such that analysis of the dwell averaged data in terms of a slowly

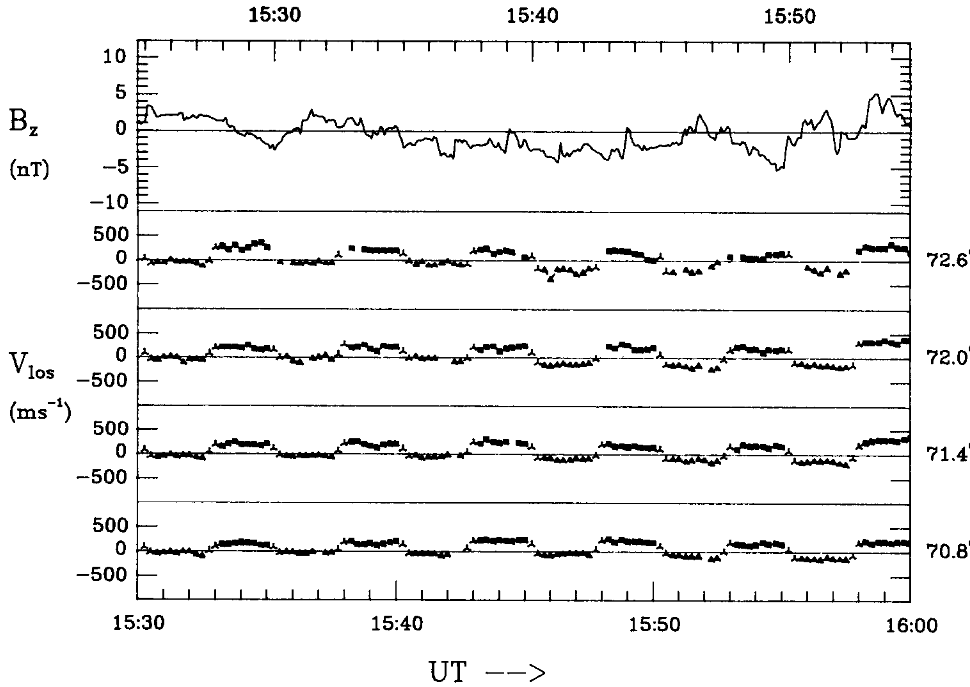

Fig. 2. Plot illustrating the format of the 15 s EISCAT 'Polar' data to be employed throughout this paper. The lower four panels show the l-o-s velocity components measured in the lowest four 'Polar' range gates for the half hour period from 1530 to 1600 UT (1800–1830 MLT) on 29 August 1985. As in Fig. 1, positive speeds indicate flow away from the radar. The panels are labelled by the invariant latitude of the gate concerned, while the symbols used are the same as those in the sketch on the right hand side of Fig. 1. In the present case the uncertainties in the l-o-s velocity components are estimated as 20, 30, 40 and 65 m s^{-1} for gates 1–4, respectively. The top panel shows 5 s averages of the IMF B_z field component in GSM coordinates measured by the AMPTE IRM magnetometer. This data has been shifted in time (by 5.3 min, as indicated by the upper UT scale) to take account of the propagation time of the IMF signal from the spacecraft to the subsolar magnetopause.

varying, uniform flow as described above (and by Willis *et al.*, 1986) may be expected to yield meaningful results. In the following sections we also show examples where this is clearly not the case. In the interval shown in Fig. 2, analysis of the dwell averaged data for gate 2, for example, indicates a flow speed of 550 m s^{-1} at azimuth 84° at the beginning of this interval, increasing to 1150 m s^{-1} at azimuth 89° at its end. Here, and throughout the paper, the flow azimuth is defined such that azimuth 0° corresponds to flow towards magnetic north, along the bisector of the two dwell directions (344° geographic), while +90° and −90° represent flow directly to the (magnetic) west and east, respectively.

Despite the above remarks concerning the consistency of the data in Fig. 2, close inspection shows that variations in V_{los} do in fact occur on time scales comparable with or shorter than the experiment cycle time, but in this case they are of rather low amplitude. Since the presence or absence of such variations and their time scales and amplitudes are the principal focus of the sections below, it is important to consider the magnitude of the experimental uncertainty in the V_{los} values. These uncertainties depend mainly on the signal to background ratio of the data, and have been estimated here from an empirical relationship which has been determined from the 'Polar' data. Specifically, in order to improve the duty cycle of the experiment, observations are made at five independent transmitter frequencies. Usually these data are averaged together before physical parameters are derived, but can be analysed separately to give five independent estimates of parameters for a given interval of time. An empirical relationship between the scatter in these single frequency estimates of l-o-s velocity and the signal to background ratio has been established which can be used to determine the uncertainties in the data presented here. For the data shown in Fig. 2 the l-o-s velocity uncertainties in gates 1–4 estimated on this basis are 20, 30, 40 and 65 m s^{-1}, respectively. By comparison, the symbols used to plot the data have widths of about $100 \mathrm{~m~s^{-1}}$. Consequently, those variations which have amplitudes comparable with or larger than the symbol size are certainly real, at least for this section of the data. V_{los} uncertainty estimates are routinely given below in the captions to each of the figures.

The final comments on Fig. 2 concern the IMF data displayed in the top panel. The component most germane to our study is the GSM north–south (B_z) component, and this is shown with 5 s resolution as measured, in this case, by the fluxgate magnetometer experiment on the AMPTE IRM spacecraft (LÜHR *et al.*, 1985). (All three GSM field components, however, are shown at lower resolution in the overview plots in Figs. 3 and 5.) The important point to note about these data (and the data in Figs. 4 and 6) is that a shift of a few minutes has been introduced between the IMF and 'Polar' data in order to take account of the propagation delay of the IMF signal from the spacecraft to the subsolar magnetopause. This shift can be seen in the UT scales marked on the upper and lower borders of the figure, where the upper scale refers to the IMF data and the lower scale to the 'Polar' data. The delay has been carefully estimated using the method described by ETEMADI *et al.* (1988), knowing the location of the spacecraft and taking into account the slowing of the flow across the bow shock and in the magnetosheath. The location of the bow shock and magnetopause were calculated from the empirical models of FAIRFIELD (1971), FORMISANO *et al.* (1979) and FORMISANO (1979), using the solar wind bulk speed and density measured *in situ* by the IRM fast plasma analyser (data kindly supplied by Dr G. Paschmann). On this basis ETEMADI *et al.* (1988) estimate delays of 6.8 min for 27 October 1984 and 5.3 min for 29 August 1985, which may be taken as constant over the whole of each experiment. It should be noted that any additional delay between corresponding features in the 'Polar' and IMF data sets must then be ascribed to the signal propagation time from the magnetopause to the 'Polar' field-of-view.

3. FLOW OBSERVATIONS ON 27 OCTOBER 1984

In order to set in context the 15 s 'Polar' data to be discussed here, we first show in Fig. 3 an overview of the large scale vector flows observed on this day, determined from the dwell averaged, beam-swinging data analysed as outlined in the previous section (see also WILLIS *et al.*, 1986). To reduce congestion in this figure only every other vector has been plotted, thus reducing the resolution to 5 min, and the predominantly east–west directed flow vectors have all been rotated clockwise through 90° such that a westward flow vector points upward, a northward flow vector to the right (as indicated), while an eastward flow vector points downward. The vectors thus actually point in the direction of the ionospheric electric field associated with the flow. A vector is plotted for a given dwell and given gate provided that the signal to background ratio exceeds 0.8%. In the dayside sector, where *F*-region densities are relatively high, eight gates are generally present spanning the latitude range 70.8°–74.9°, but this number is reduced to five or six at night. Shown above the 'Polar' data are 1 min averages of the IMF in GSM coordinates, obtained simultaneously by the AMPTE UKS magnetometer (SOUTHWOOD *et al.*, 1985) during the interval between about 0600 UT and 1500 UT (no time shifts relative to the 'Polar' data have been introduced into this lower resolution plot). The principal feature of interest in these data is that, over the interval observed, the IMF B_z component is predominantly positive prior to 1107 UT, when it turns abruptly negative and remains mostly negative from then onwards. The K_p values for the interval 0000–1500 UT are 2_0, 2+, 2+, 2− and 3−. This indicates a relatively quiet period overall, as might be expected from the northward orientation of the IMF, but there is an increase in magnetic activity towards the end of the experiment which is presumably associated with the southward turning of the field.

Looking now at the 'Polar' flow data, it can be seen that four principal regions can be identified. With increasing local time these are the dawn auroral zone flow cell, a region of weak sporadic flows spanning the midday hours, the dusk auroral zone flow cell and the evening polar cap boundary region of weak flows. These regions will now be described in greater detail. At the beginning of the experiment in the early morning hours (starting at about 0200 MLT) strong, predominantly eastward flows are observed for about the first 3 h which correspond to the dawn cell of the usual auroral zone flow. Short intervals of westward flow are also observed during this period, presumably indicating that polar cap flow has extended into the radar viewing area. Between 0230 and 0310 UT (0500 and 0540 MLT) the region of fast eastward flow recedes poleward across the field-of-view and only weaker, more sporadic flows are then observed, which are predominantly eastward before about 0600 UT (0830 MLT) and westward thereafter. At about 1120 UT (1350 MLT) a major enhancement in westward flow occurs simultaneously across the entire Polar latitude range, which is associated with the

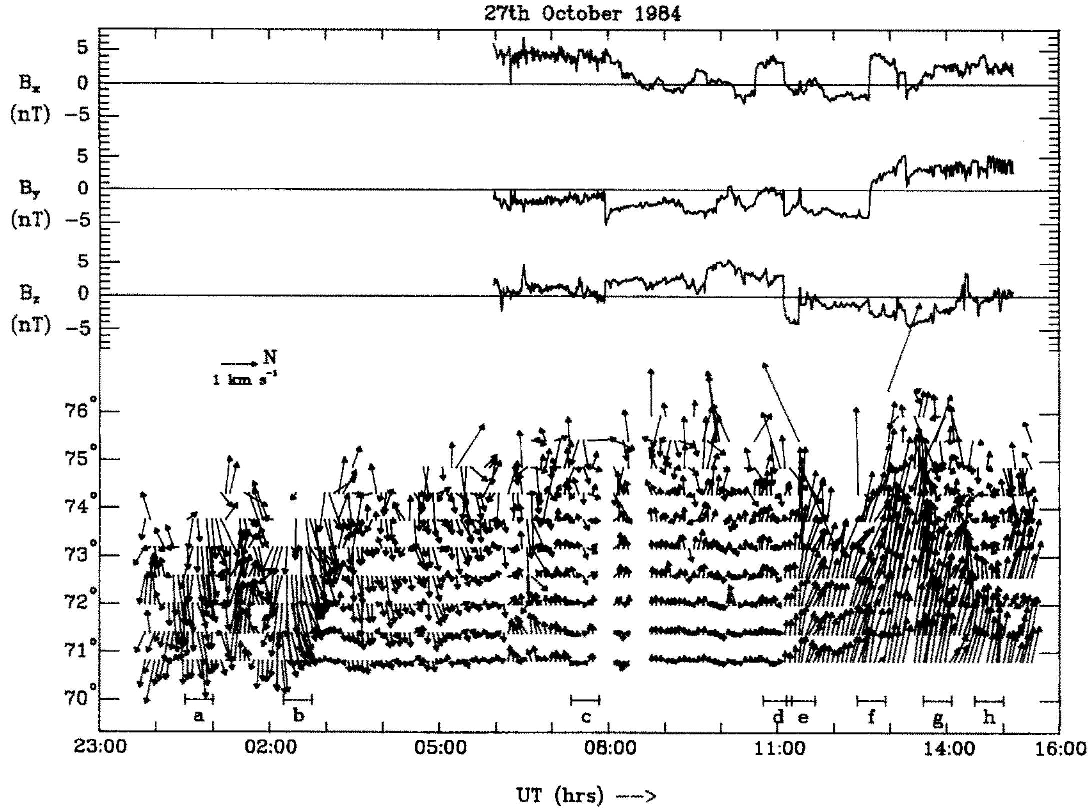

Fig. 3. Overview plot of the EISCAT Polar ionospheric flow and AMPTE UKS IMF measurements made on 27 October 1984. The IMF measurements are 1 min averages in GSM coordinates, with no time lag introduced. The ionospheric flow vectors were determined from the 'Polar' beam-swinging data and are shown with 5 min resolution. These vectors have been rotated clockwise by 90° to avoid congestion. The horizontal bars marked a–h at the bottom of the plot show the half hour intervals which have been selected to illustrate the 15 s data in Fig. 4.

southward turning of the IMF observed at 1107 UT (note the propagation delay of about 7 min from the UKS to the dayside magnetopause discussed in the last section). This sudden onset has been described in detail by RISHBETH *et al.* (1985), LOCKWOOD *et al.* (1986) and WILLIS *et al.* (1986). The flow remains strong and directed to the north-west, corresponding to the dusk auroral zone flow cell, until about 1330 UT (1600 MLT), when it starts to weaken and turn more directly westward at the more northerly latitudes sampled. This feature heralds an entry of the radar viewing area into a rather diffuse boundary region of weak irregular flows between the dusk auroral zone cell and the polar cap. As time increases, the region of weakened flow expands across the field-of-view, although the flow remains strongly westward in the lower gates until the end of the experiment at 1530 UT (1800 MLT).

The horizontal bars in Fig. 3 marked a–h indicate the half hour intervals we have selected for presentation in Fig. 4 to illustrate the nature of the 15 s flow data observed in the various regions identified above. Fig. 4(a) shows 15 s data plotted in the format described in Section 2 for the interval 0030–0100 UT (0300–0330 MLT), corresponding to the early morning flows in the dawn auroral zone cell (no IMF data are available for this interval). It can be seen that although the flows are consistently eastward directed over most of the period (triangles positive, squares negative), in agreement with Fig. 3, a considerable degree of irregularity is also present. This may be contrasted, for example, with the smooth, steady flows already exhibited in Fig. 2. Variations in the l-o-s velocity component of about 200 m s^{-1} occur over 30 s, with even larger changes up to 500 m s^{-1} occurring over the 5 min between successive dwells at the

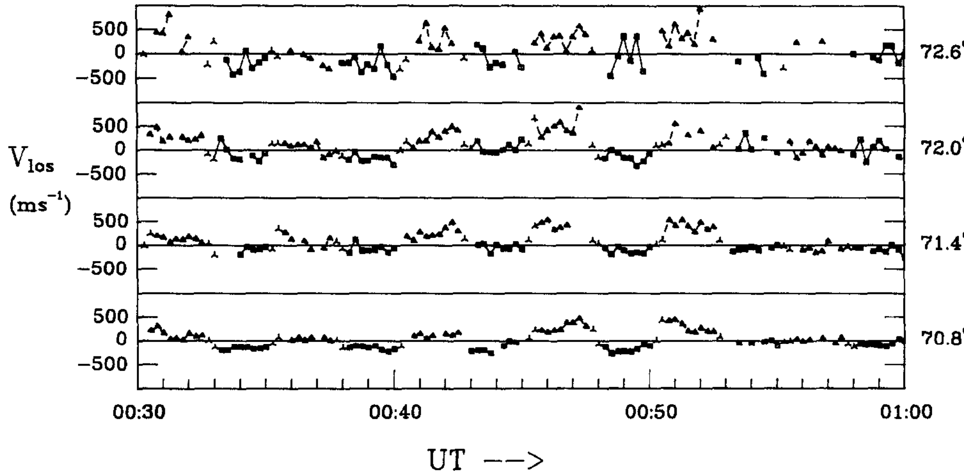

Fig. 4(a). As for Fig. 2, except for the period 0030–0100 UT (0300–0330 MLT) on 27 October 1984. No IMF data are available for this period. The uncertainties in the l-o-s velocity components are 40, 75, 95 and 145 m s^{-1} for gates 1–4, respectively.

same azimuth. Estimates of the uncertainties in these values for this section of data are 40, 75, 95 and 145 m s^{-1} for gates 1–4, respectively, such that although the main variations on the above scales observed in the lower gates are real, those occurring in the higher gates are also due in part to noise. This is also apparent from visual inspection of the data. Figure 4(a) thus shows that the nightside flow data have a characteristically ragged appearance, indicative of the presence of irregular variations of bulk flow speed and/or direction over a range of time scales from about 30 s to 10 min. Clearly, the 2.5 min vectors derived from the beam-swinging data can only represent the longer period variations in such flows. During the interval presented here the vectors derived on this basis are generally directed within 10° of due east (azimuth −90°), but the speed varies widely between ~300 and ~1200 m s^{-1} (see Fig. 3).

As the radar rotates toward the dawn meridian, the 'Polar' field-of-view moves towards the equatorward portion of the dawn flow cell. In this regime the l-o-s flows become somewhat smoother on the shorter time scales (1 min or less) but tend to undulate in value on time scales of a few minutes with amplitudes of a few hundred metres per second, suggestive of the presence of ULF pulsations. Figure 4(b) shows 15 s data for the interval 0215–0245 UT (0445–0515 MLT), where the equatorward 'edge' of the dawn flow cell starts to move poleward across the viewing area. Undulations in the l-o-s components are evident during the first part of this interval, particularly in the lower gates, but it is clear that much of the short period variability in gates 3 and 4 is due to noise (uncertainties for gates 1–4 are 25, 55, 130 and 245 m s^{-1}, respectively). With regard to the large scale flow, the pattern of behaviour observed in each gate is similar, but is delayed in the higher gates relative to the lower gates. The predominantly eastward flow turns toward the north and then smoothly declines in strength over half an hour. This process is essentially complete for gate 1 at the end of the interval shown (the flow speed for this gate determined from the beam-swinging data declines from about 400 to 100 m s^{-1} over this interval). Similar conditions of nearly zero flow (both in terms of net convection and oscillations) are reached after successive 10 min intervals in successively higher gates. While this process is in progress, a substantial velocity shear exists across the radar field-of-view. For example, near the beginning of the interval shown in Fig. 4(b), the speed increases from a few hundred metres per second in gate 1 to over 2 km s^{-1} in gate 4 (the direction of the latter flow being within a few degrees of due east).

After the dawn flow cell has receded poleward of the field-of-view, the background flows remain small for the following 8 h, although weak sporadic flows do occur in this period, sometimes with oscillations superposed whose period is several minutes, comparable with the beam-swinging cycle time. A major feature of the data in this interval, however, is the occurrence of remarkable, short lived 'flow burst' events, four clear examples of which occur on this day at about 0611, 0636, 0641 and 0736 UT. The first of these shows a brief 1–2 min burst of poleward flow

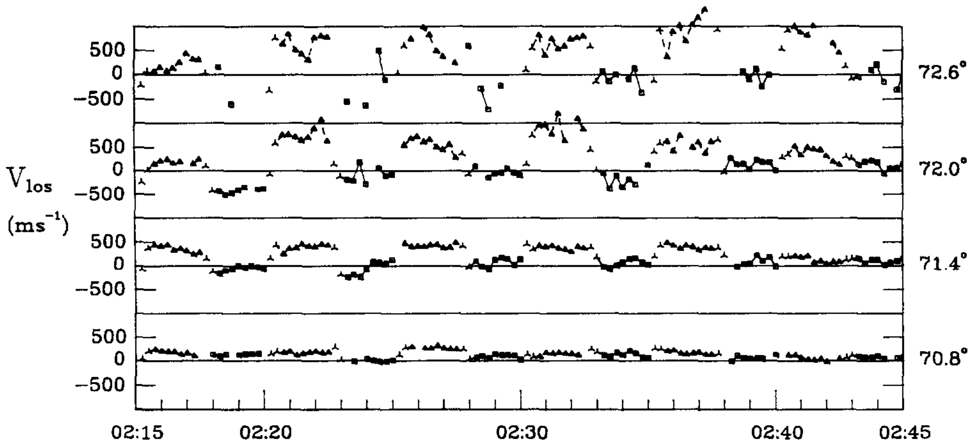

Fig. 4(b). As for Fig. 2, except for the period 0215–0245 UT (0445–0515 MLT) on 27 October 1984. No IMF data are available for this period. The uncertainties in the l-o-s velocity components are 25, 55, 130 and 245 m s^{-1} for gates 1–4, respectively.

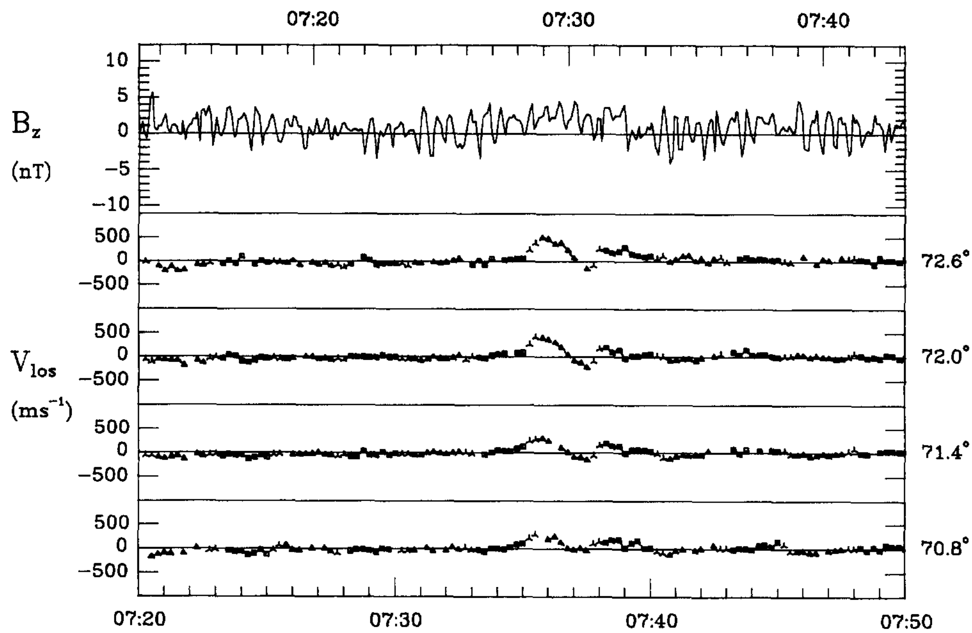

Fig. 4(c). As for Fig. 2, except for the period 0720–0750 UT (0950–1020 MLT) on 27 October 1984. The uncertainties in the l-o-s velocity components are 30, 25, 35 and 90 m s^{-1} for gates 1–4, respectively. In this plot the IMF data have been shifted by 6.8 min relative to the 'Polar' data.

which is seen only in the higher gates, while the second and third have been described in detail by TODD *et al.* (1986) and are not discussed further here. Instead, in Fig. 4(c) we show the interval 0720–0750 UT (0950–1020 MLT) encompassing the fourth event. It can be seen that the flows are very small for a considerable period both before and after the event, illustrating how weak the dayside ionospheric flows can be under conditions of a small northward component of the IMF. However, towards the end of the dwell at azimuth 1 (squares) at about 0734 UT a small but increasing positive l-o-s component is present. On returning to azimuth 2 (triangles) at about 0736 UT, large poleward flows are then observed which are larger at higher latitudes, peaking at about 800 m s^{-1} in gate 7 (not shown). These flows decline sharply during the dwell, reaching zero l-o-s speed and later reversing in sign successively with increasing latitude. Essentially similar behaviour was described by TODD *et al.* (1986) for the events observed earlier on this day. Finally, on returning to azimuth 1 at about 0738 UT smaller positive flows are still observed, though they decline essentially to zero during the dwell. It is intriguing to note that the IMF data in the figure appear to indicate that the burst is associated with a brief interval of stronger northward field, as is in fact also true of the events discussed by TODD *et al.* (1986). However, since the flow burst occurs with essentially no delay following the estimated arrival of the northward field at the subsolar magnetopause (also true of the Todd *et al.*, events), the significance of this observation and the causal connection remain unclear at the present time. There are no related changes in either the solar wind flow speed or density. (Note that the 40 s oscillations seen in the IMF data are probably foreshock 'upstream waves'.)

Figures 4(d) and 4(e) present the 15 s data which encompass the sudden appearance at 1120 UT of the westward flows of the dusk cell, resulting from a southward turn of the IMF at 1107 UT. The interval immediately preceding the flow onset, between 1045 and 1115 UT (1315–1345 MLT) when the (shifted) IMF is nearly continuously northward, is shown in Fig. 4(d). This data illustrates the weak oscillations (of about 100 m s^{-1} amplitude) which often occur in the 'Polar' data under these conditions in the region of low dayside flows between the dawn and dusk flow cells. Similar, smooth, quasi-sinusoidal variations are observed in all four gates, and at both azimuths. The period of the oscillation in this case is about 5 min, approximately equal to the experiment cycle time. The result of analysing such data using the usual beam swinging algorithm is generally to produce flow vectors of modest amplitude [e.g., about 50 m s^{-1} during the first half of Fig. 4(d)] and rather variable direction. However, if the wave period and the experiment cycle times are similar, as seems to be the case in the present example, then 'beating' between the two can give rise to spurious, low amplitude, slowly modulated flows in the vector data.

Figure 4(e) then shows data for the interval 1110–1140 UT, which, for clarity of presentation, overlaps the data shown in the previous figure by 5 min. It can be seen that an enhanced flow is first observed in all gates at azimuth 1 (squares) starting at 1119 UT, approximately 5 min after the southward IMF observed by AMPTE UKS arrived at the magnetopause. This flow is initially mainly westward (680 m s^{-1} at azimuth 84° in the lower gates at 1123 UT), but acquires a significant tilt towards the north after several minutes (510 m s^{-1} at 65° in gates 1 and 2 at 1133 UT). Flow speeds are generally higher at higher latitudes (varying, for example, between 510 m s^{-1} in gate 1 and 750 m s^{-1} in gate 4 at 1133 UT), suggesting that the radar field-of-view corresponds to the equatorward portion of the dusk flow cell which is excited by the reconnection-induced coupling at the magnetopause. The outstanding feature of the 15 s data after the enhancement, however, is their smooth appearance, both from point to point and dwell to dwell, suggestive of a very smooth, laminar flow. Clearly, the flow vector estimates obtained from the beam-swinging data should represent excellent approximations under such circumstances.

As time progresses and the radar rotates into the mid-afternoon sector, the speed of the north westward directed convective flow increases. Low amplitude oscillations with periods of a few minutes reappear after 1145 UT (1415 MLT), with peak to peak variations in the l-o-s components of about 200 m s^{-1}. Their amplitude thus remains generally smaller than the values associated with the background flow. However, intervals of much larger amplitude, wave-like perturbations also occur in this region. These perturbations appear to have an impulsive, 'bursty' character, and can reach peak to peak amplitudes along the l-o-s in excess of 500 m s^{-1}, such that the change in the l-o-s velocity component during a dwell period can become comparable with or larger than the average value. An example of this type of behaviour is shown in Fig. 4(f), which displays 15 s data for the interval 1225–1255 UT (1455–1525 MLT). Variations in the l-o-s components during each dwell are relatively modest at both the beginning and end of this interval, but become very large indeed in all gates during the 10 min interval between about 1236 and 1246 UT. (The uncertainties in the l-o-s components are only 35, 50, 80 and 130 m s^{-1}.) Qualitatively, the form and amplitude of these perturbations are not dissimilar to those occurring in 'flow burst' events, and it is tempting to speculate on a possible common origin (in terms, for example, of impulsive magnetopause coupling processes). However, unlike the earlier flow bursts on this day, the IMF remains southward during this interval. We therefore find that, as in the case of the early morning dawn flow cell data

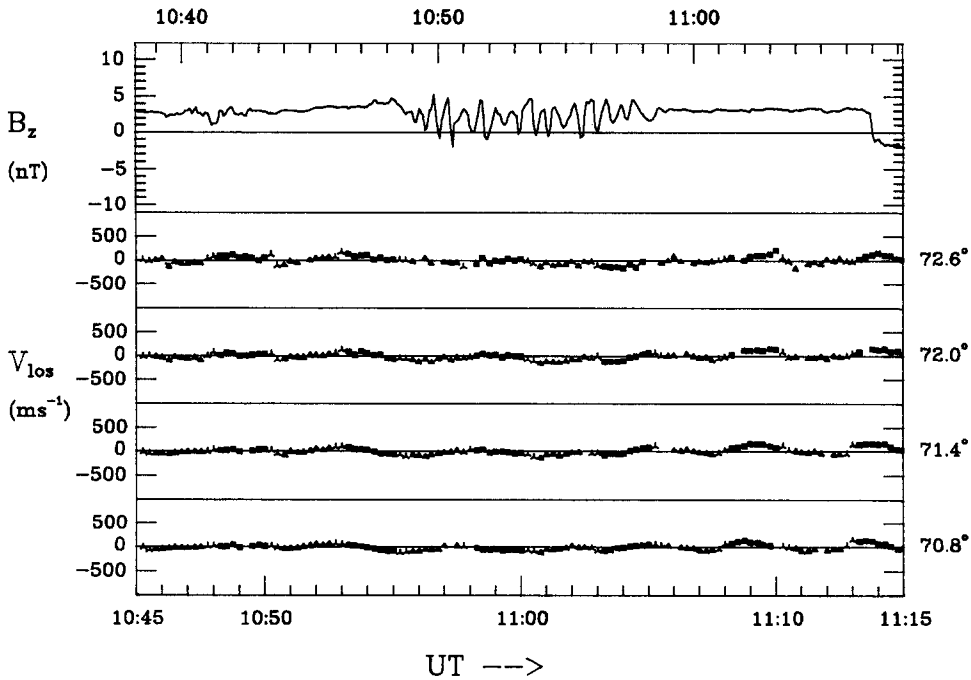

Fig. 4(d). As for Fig. 2, except for the period 1045–1115 UT (1315–1345 MLT) on 27 October 1984. The uncertainties in the l-o-s velocity components are 15, 15, 30 and 50 m s^{-1} for gates 1–4, respectively. In this plot the IMF data have been shifted by 6.8 min relative to the 'Polar' data.

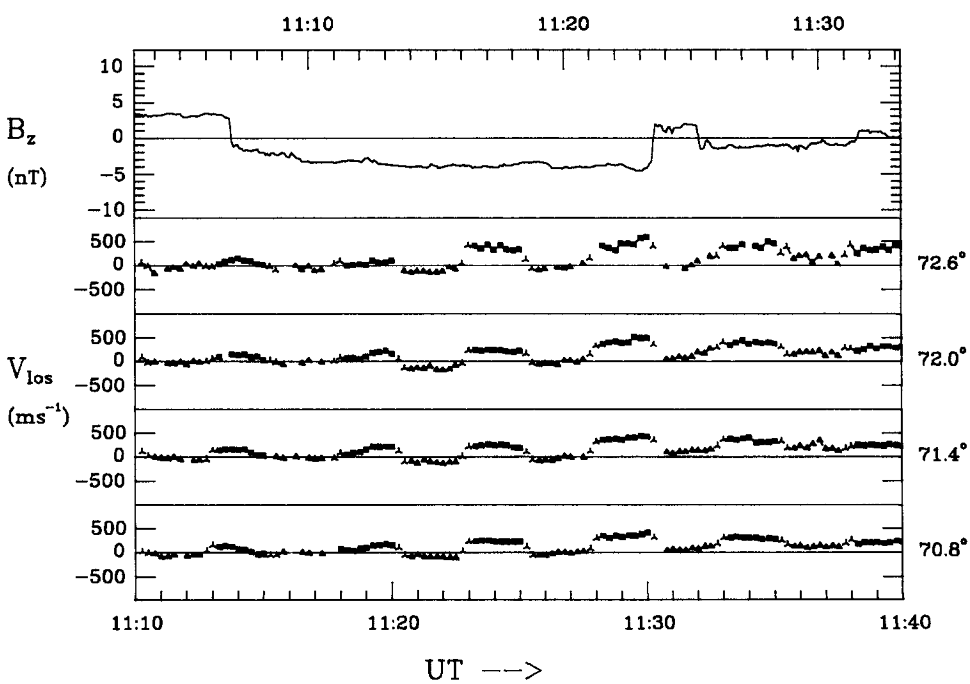

Fig. 4(e). As for Fig. 2, except for the period 1110–1140 UT (1340–1410 MLT) on 27 October 1984. The uncertainties in the l-o-s velocity components are 15, 20, 35 and 65 m s^{-1} for gates 1–4, respectively. In this plot the IMF data have been shifted by 6.8 min relative to the 'Polar' data.

discussed above [Fig. 4(a)], large amplitude flow irregularities occur in the central portion of the dusk flow cell in the mid-afternoon hours. The character of the irregularities appears to be different in the two cases, however, taking the form of impulsive, wave-like disturbances with periods of a few minutes in the afternoon dusk cell, but being far more irregular and containing variations with time scales from about 30 s–10 min in the early morning dawn cell.

Flows remain similar to those shown in Fig. 4(f) for the next hour, until the poleward edge of the dusk cell and the polar cap boundary region move into the northern part of the 'Polar' field-of-view. With increasing distance to the north in this region, the strong, wavy, north-westward flows of the central dusk flow cell give way to weaker, smoother and more westward directed flows at the cell's poleward edge. The flows decrease in magnitude essentially to zero within the polar cap boundary itself. As the radar rotates towards the dusk meridian, these boundary regions expand across the 'Polar' field-of-view, such that the above pattern of behaviour is seen in each of the gates in turn, at successively later times at lower latitudes. Consequently, during this interval the latitudinal gradient of the westward flow reverses in sense compared with that observed in the early afternoon sector, the flows now being weaker with increasing latitude. This feature is clearly present in the data shown in Fig. 4(g) for the period 1335–1405 UT (1605–1635 MLT). The flows are large (about 1500 m s^{-1} at azimuth 80°) and exhibit considerable wave activity in the lower two gates, but are weaker (750 m s^{-1} at azimuth 76°) and smoother in gates 3 and 4. Later, smooth flows of moderate amplitude are observed in all four gates, as shown in Fig. 4(h) for the interval 1430–1500 UT (1700–1730 MLT). Here the l-o-s speeds in the two azimuths show only small variations from point to point and from dwell to dwell. In the middle of the interval shown (1445 UT) the flow speed and azimuth varies from approximately 900 m s^{-1} and 80° in gate 1 to 500 m s^{-1} and 100° in gate 4. The flows then remain of a similar character in the 'Polar' field-of-view until the end of the experiment just after 1530 UT (1800 MLT), which occurs before entry into the polar cap proper.

4. FLOW OBSERVATIONS ON 29 AUGUST 1985

We now consider the simultaneous EISCAT 'Polar' and IMF observations made on 29 August 1985, and in Fig. 5 we first present an overview of the data in the same format as Fig. 3. The 'Polar' observations on this day cover the period from 1002 to 1850 UT (approximately 1230–2120 MLT), corresponding to the post noon to evening local time sector. The data do not therefore encompass as long an interval as on 27 October 1984 discussed above, but do extend the coverage past the dusk meridian. IMF data were obtained from the AMPTE IRM spacecraft from 1030 to 1700 UT and so cover much of the 'Polar' run. Comparison of the IMF data with that for 27 October 1984 in Fig. 3 shows that the field direction is very much more variable on this day. The principal feature of the IMF data on 27 October 1984 is a single sharp switch from northward to southward fields which occurs when EISCAT is in the early afternoon sector, with effects in the flow data which have been discussed above. On 29 August 1985 the field is generally northward during the experiment, though punctuated by frequent, relatively brief southward excursions, of typically 10 min duration. It is shown below that, although the flows observed on this day have basic similarities with those observed at similar local times on 27 October 1984, significant differences also occur which can be related directly to the IMF behaviour. Geomagnetically, this interval is rather more disturbed than on 27 October 1984, with K_p values for 0900–2100 UT of 3 −, 4 −, 3_0 and 4.

The vectors in the lower half of Fig. 5, determined from the 'Polar' beam-swinging data, give an overview of the flows observed on this day, and can again be divided into four basic regions. These are the midday region of low flow speeds, the dusk auroral zone flow cell, the polar cap boundary region (all also observed on 27 October 1984), and finally a region of predominantly equatorward flow observed in the evening polar cap. In more detail, the dayside region of low convective flows is observed from the start of the experiment just after 1000 UT until about 1115 UT (1230–1345 MLT). Although the flow speeds are generally small in this region, Fig. 5 does in fact indicate some sporadic flows with vectors of variable amplitude and direction, the origins of which will become apparent when the 15 s l-o-s components are examined. After about 1115 UT the flows remain continuously north-westward across the field-of-view for the next 4.5 h (1345–1815 MLT), corresponding to the main part of the dusk auroral zone flow cell. Weaker, variable flows then spread intermittently across the 'Polar' viewing area from the north as the boundary of the polar cap is encountered, encompassing the entire field-of-view by about 1700 UT (1930 MLT). As noted in the previous section, a very similar feature was observed on 27 October 1984, but starting about 2 h earlier in local time. These weak flows persist until about 1800 UT (2030 MLT), when steadily growing polar cap flows are observed, which are directed

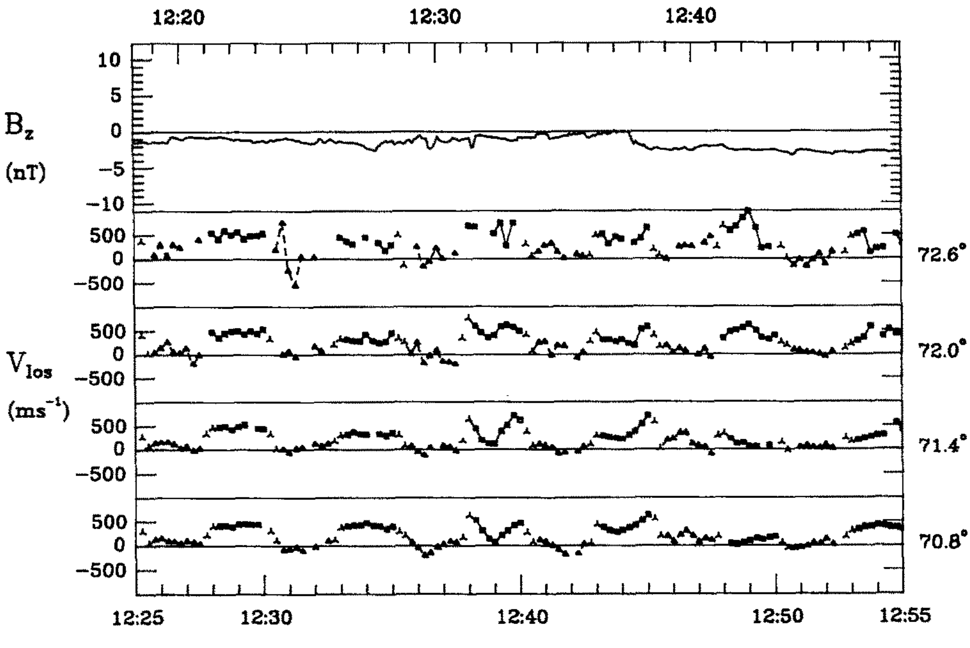

Fig. 4(f). As for Fig. 2, except for the period 1225–1255 UT (1455–1525 MLT) on 27 October 1984. The uncertainties in the l-o-s velocity components are 35, 50, 80 and 130 m s^{-1} for gates 1–4, respectively. In this plot the IMF data have been shifted by 6.8 min relative to the 'Polar' data.

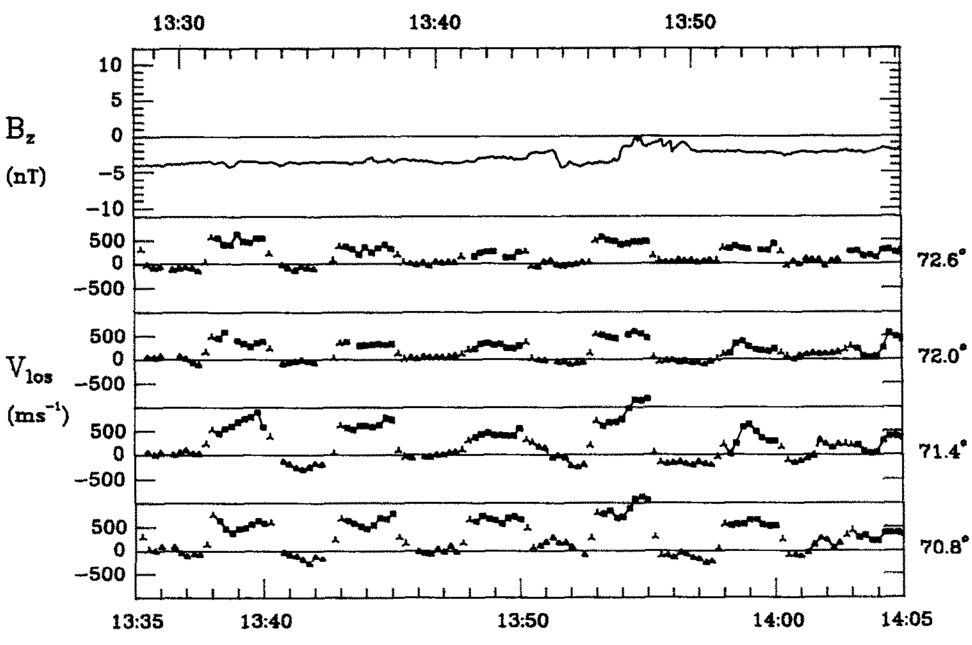

Fig. 4(g). As for Fig. 2, except for the period 1335–1405 UT (1605–1635 MLT) on 27 October 1984. The uncertainties in the l-o-s velocity components are 50, 35, 30 and 50 m s^{-1} for gates 1–4, respectively. In this plot the IMF data have been shifted by 6.8 min relative to the 'Polar' data.

equatorward until the end of the experiment at 1850 UT (2120 MLT).

The horizontal bars marked a–f in Fig. 5 again indicate the half hour intervals selected to represent the 15 s 'Polar' data observed on this day, which will now be presented in Fig. 6. The horizontal bar marked 2 indicates the interval already presented in Fig. 2, which was used to introduce the data format in Section 2, and is briefly discussed here in context.

At the beginning of the experiment, for the first 15 min, the l-o-s flows indicate the presence of a weak ($\sim$100–200 m s^{-1}) northward drift, which is modulated by weak oscillations of the characteristic few minutes period, almost 100 m s^{-1} in amplitude. These observations indicate that the viewing area is located in the dayside region of low flows between the main auroral zone flow cells at 'Polar' latitudes, though at the same local time on 27 October 1984 the ionosphere was quite still (to within a few tens of metres per second), both in terms of convective and oscillatory flows. At about 1020 UT, a remarkable damped wave train is then observed which is shown in Fig. 6(a). This figure spans the interval 1010–1040 UT (1240–1310 MLT) and shows that the wave appears to be impulsively generated at about 1018 UT, beginning with small negative l-o-s velocities (towards the radar) in gates 1–4, but increasing with latitude to much larger negative values (about 500 m s^{-1}) in gates 5 and 6 (not shown). The initial amplitude in gate 1 is about 500 m s^{-1}, being somewhat larger at higher latitudes, and decays over three cycles to the pre-existing $\sim$100 m s^{-1} amplitude level. It is the occurrence of this wave which gives rise to the relatively large, irregularly directed vectors at the start of the flow map in Fig. 5. Clearly, these vectors do not give an adequate representation of the actual ionospheric flows during this interval, depending as they do on the arbitrary relative phases of the wave and the beam-swinging experiment.

This wave has similarities to the 'flow burst' events described above, and also appears to be directly related to the transient pulsations which have been observed in ground magnetometer and STARE radar data (POULTER and NIELSEN, 1982; POULTER et al., 1984; ALLAN and POULTER, 1984; ALLAN et al., 1985, 1986). These waves represent damped eigen-oscillations of the field lines which are excited by an impulsive, broad-band source, such that the wave period increases with increasing latitude. The nature of the impulsive excitation remains unclear, however, and

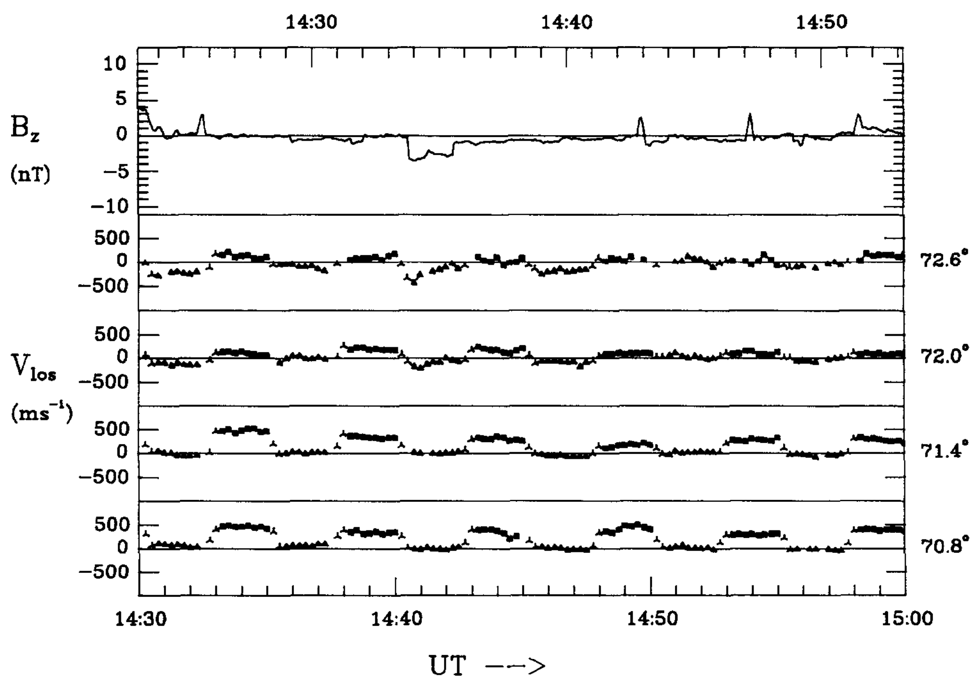

Fig. 4(h). As for Fig. 2, except for the period 1430–1500 UT (1700–1730 MLT) on 27 October 1984. The uncertainties in the l-o-s velocity components are 20, 20, 30 and 50 m s^{-1} for gates 1–4, respectively. In this plot the IMF data have been shifted by 6.8 min relative to the 'Polar' data.

unfortunately in the present case no concurrent AMPTE IRM data are available to determine whether the wave onset is related to features in the solar wind or IMF. It is also difficult to tell from Fig. 6(a) whether the wave period changes significantly over the latitude range. Judging from the second zero crossing observed in azimuth 1, which occurs 30 s later in gate 4 than in gate 1, there seems to be some increase, by approximately 15 s per degree of latitude, but this is rather less than values reported by the authors referenced above.

By the end of the period shown in Fig. 6(a), the flows have returned to a slow, modulated northward drift of about 200 m s^{-1}, similar to that observed at the beginning of the interval. These flows then gradually decay to even smaller values, reaching essentially zero flow in gate 1 and about 100 m s^{-1} to the north in gate 4 by 1100 UT (1330 MLT). This decline takes place in the presence of a strongly positive IMF B_z component ($\sim$4 nT, see Fig. 5), measurements of which are available after 1032 UT. At about 1110 UT a weak, smooth north-westward (azimuth $\sim$70°) flow reappears across the field-of-view, whose onset appears to be associated with a reduction in the IMF B_z component from 5 to 3 nT at 1059 UT (see Fig. 5). The flow speeds increase with increasing latitude (from $\sim$200 m s^{-1} in gate 1 to $\sim$500 m s^{-1} in gate 4 at 1120 UT) suggesting that the field-of-view encompasses the equatorward border of the dusk flow cell. The value of B_z then declines further and is southward for the brief interval between 1118 and 1122 UT, after which it becomes positive again. The apparent ionospheric response to the interval of southward IMF is a burst of rapid poleward flow which begins at 1129 UT, 5 min after the southward field reaches the magnetopause. This flow burst is displayed in Fig. 6(b), which shows data for the interval 1120–1150 UT (1350–1420 MLT). It can be seen that the burst begins at the same time in all gates (to within 15 s), and after 45 s reaches a peak speed along the l-o-s of about 900 m s^{-1} in gate 1, rising to about 1.2 km s^{-1} in gate 4. After the onset the mean flow then declines to smaller values over about 10 min, presumably because of the short-lived nature of the southward turning, but superimposed upon the decline is a damped wave train with characteristics similar to those of the wave observed earlier and displayed in Fig. 6(a). We suggest that this wave represents the damped, transient response of the system to the impulse in flow excited by the southward turning of the IMF. It should be noted that there is no indication in the IRM plasma data of changes in solar wind bulk speed or density at this time. It may seem remarkable that a brief southward turning of the field can lead to such a striking response in the ionospheric flows, and taken as an isolated instance the apparent correlation might be seen as coincidental. However, the very close correspondences we have found in detailed examination of the 'Polar'/AMPTE data taken as a whole (only a small part of which is presented in this paper) convince us that these correlations are real. After the impulsive flows shown in Fig. 6(b) have died away, by about 1140 UT, moderate, relatively smooth, north-westward flows remain which are clearly enhanced compared with those occurring previously (e.g. in gate 2 from 350 m s^{-1} at azimuth 76° at 1120 UT to 550 m s^{-1} at azimuth 72° at 1145 UT). Similarly-directed flows of variable amplitude are then observed continuously for about the next 4 h as the radar traverses the dusk auroral zone flow cell. Thus, neglecting the very weak flows observed just before the burst, entry into the dusk cell proper on this day was initiated by the flow burst shown in Fig. 6(b). On both days discussed in this paper, therefore, entry into the dusk cell is a temporal event controlled by the north–south component of the IMF, rather than a spatial phenomenon related to the rotation of the radar under a steady ionospheric flow pattern. To observe the latter, the IMF would have to remain steady for a period of several hours as the radar rotates from noon through to dusk, while significant variations in the field usually take place on time scales shorter than this. However, despite the fact that entry into the dusk cell is due to a southward turning of the IMF on both days, and that these occur at very nearly the same local time, it can be seen that the detailed ionospheric response is different in the two examples. In the case discussed here a large impulsive poleward flow and an associated damped, transient pulsation is first observed, which is then followed by smooth, enhanced north-westward dusk cell flows. In the case discussed in the previous section, however, only the latter response is observed [Fig. 4(e)]. A plausible explanation for this difference lies in the location of the radar field-of-view relative to the ionospheric footprint of the newly open flux tubes created by reconnection at the magnetopause. Close to the latter site we may expect to see the relatively short scale effects of individual reconnection events (e.g. FTEs), which should include large, impulsive flows, together with the pulsations which these events generate on adjacent closed flux tubes. This scenario may correspond to the present example, shown in Fig. 6(b). On the other hand, if the radar field-of-view is located in the auroral zone far from the site where the newly reconnected field lines intersect the ionosphere, as we would infer for the case described in the previous section (see also LOCKWOOD *et al.* 1986), only the temporal excitation of the large scale, twin vortical

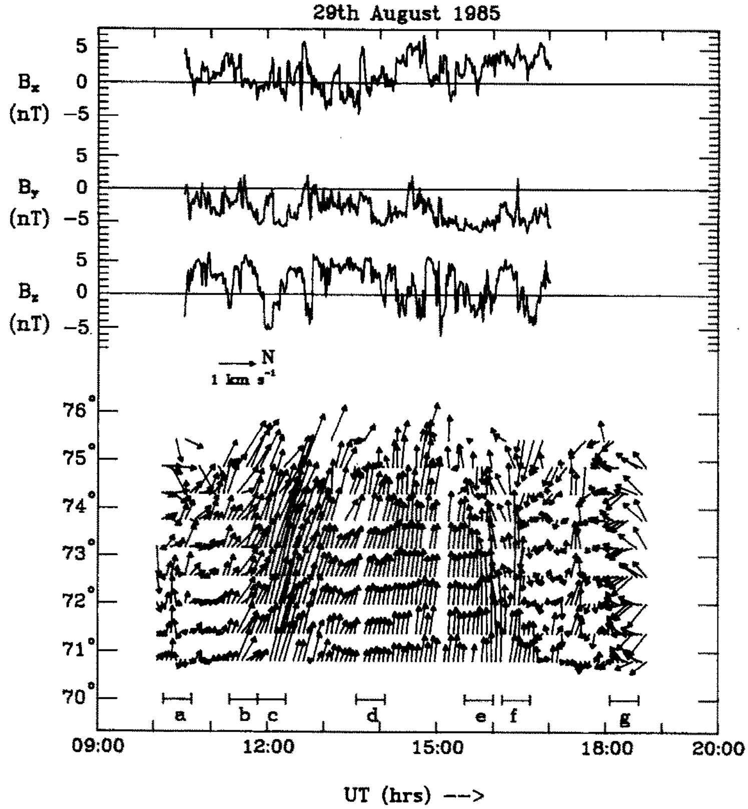

Fig. 5. Overview of the EISCAT 'Polar' ionospheric vector flows and AMPTE IRM IMF B_z measurements on 29 August 1985, in the same format as Fig. 3. The horizontal lines at the bottom of the figure marked a–f refer to Fig. 6, while that marked 2 refers to Fig. 2.

flows would be observed and not the larger amplitude, shorter range transient flows in the vicinity of the small scale individual newly opened flux tubes themselves.

As noted above, after the impulsive onset at about 1130 UT, the 'Polar' field-of-view remains continuously within the westward flows of the dusk cell until the polar cap boundary region is encountered at the northernmost latitudes sampled at about 1545 UT. However, as can be seen in Fig. 5, large variations in the north–south component of the field are observed over this interval and these lead to clear modulations of the dusk cell flow, as illustrated in Figs. 6(c) and 6(d). In Fig. 6(c) we show data for the period 1150–1220 UT (1420–1450 MLT), which directly follows the impulsive onset data shown in the previous figure. At the beginning of this interval we observe the smooth, relatively weak flows which remain after the impulsive onset, when the IMF has a strong northward component. As in the interval immediately preceding the impulse, these flows have a larger speed at higher latitudes within the radar viewing area, suggestive of a location in the equatorward part of the dusk flow cell at this time. At about 1150 UT IMF B_z declines to near zero values, and then at about 1156 UT turns strongly southward (about 5 nT) for a 10 min interval before becoming smaller in magnitude and then northward again. The ionospheric response is a clear enhancement of the flows seen after about 1205 UT, increasing in gate 2, for example, from 380 m s^{-1} (at azimuth 51°) at about 1150 UT, to 1270 m s^{-1} (at azimuth 72°) by about 1210 UT. These high speed flows are relatively smooth, particularly in the lower gates, though modulations of a few minutes of moderate amplitude are apparent in the higher gates. (The uncertainties in these flows for gates 1–4 are 20, 30, 50 and 85 m s^{-1}, respectively.) During the period of enhanced flows the latitudinal gradient evident at the beginning of the interval essentially disappears, suggestive of an expanded flow pattern and a viewing

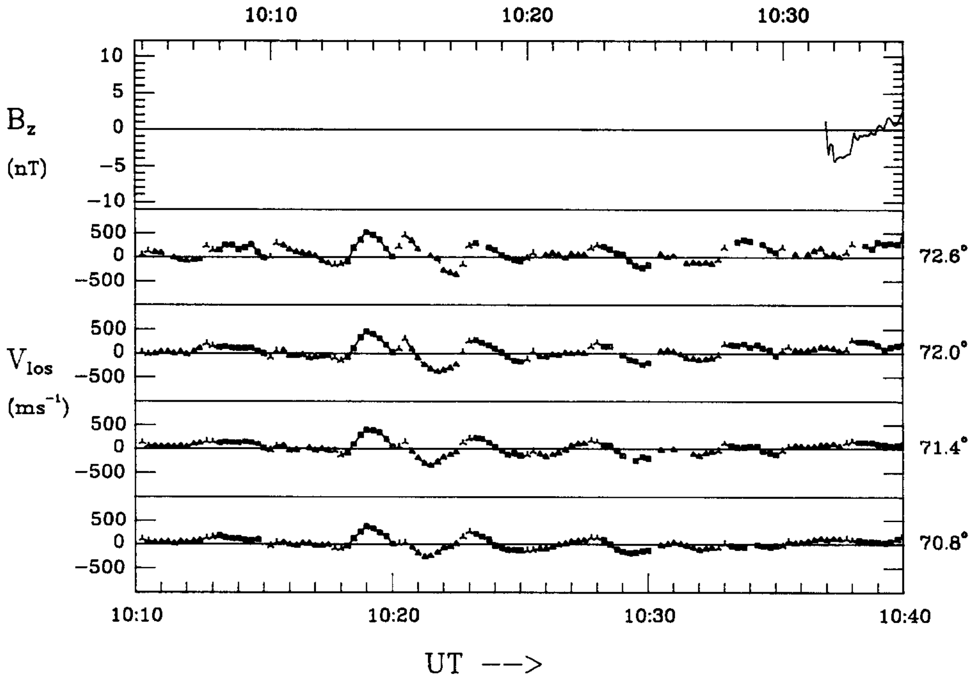

Fig. 6(a). As for Fig. 2, except for the period 1010–1040 UT (1240–1310 MLT) on 29 August 1985. The uncertainties in the l-o-s velocity components are 15, 20, 30 and 45 m s^{-1} for gates 1–4, respectively. In this plot the IMF data have been shifted by 5.3 min relative to the 'Polar' data.

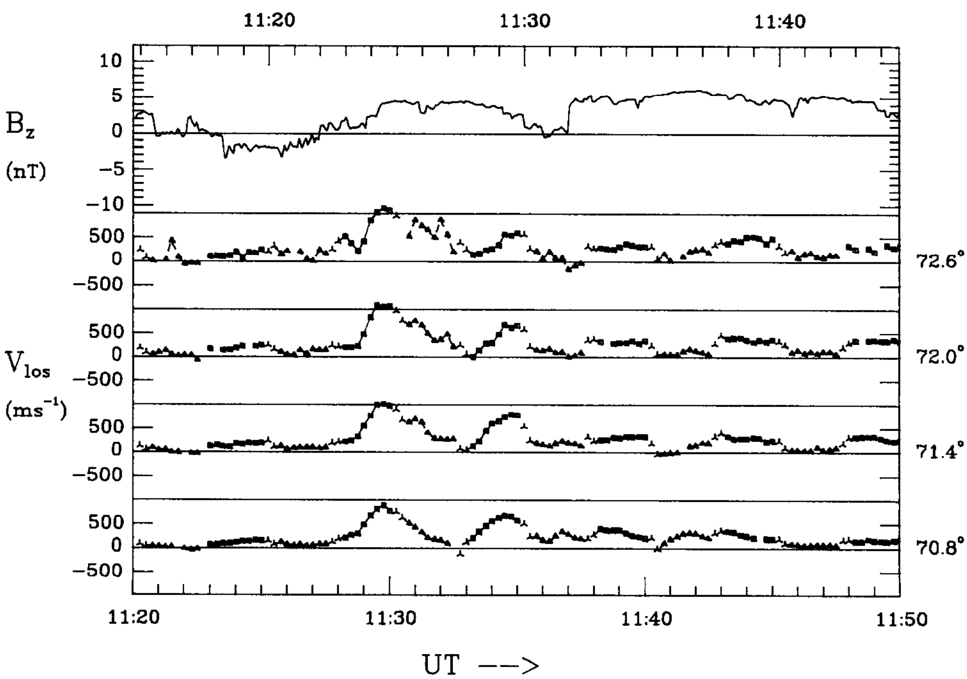

Fig. 6(b). As for Fig. 2, except for the period 1120–1150 UT (1350–1420 MLT) on 29 August 1985. The uncertainties in the l-o-s velocity components are 15, 25, 40 and 70 m s^{-1} for gates 1–4, respectively. In this plot the IMF data have been shifted by 5.3 min relative to the 'Polar' data.

area which is more centrally located within the flow cell. However, the gradient reappears again after the field once more turns northward and the flows decline at and after the end of the interval shown.

Following further IMF modulation of the flows during the half hour period subsequent to that shown in Fig. 6(c), the IMF remains consistently northward after about 1250 UT for more than an hour, until about 1400 UT. During this period the dusk cell flows persist, but become weaker than before. These flows are illustrated in Fig. 6(d), which shows data for the interval 1335–1405 UT (1605–1635 MLT). The flows are very smooth, with little point to point or dwell to dwell variation, a condition which seems to be typical of the equatorward portions of the auroral zone flow cells. To demonstrate further the IMF control of these flows, we need only compare these data with those obtained on 27 October 1984 during the same local time interval but under conditions of southward directed fields, as shown in Fig. 4(g). The flows are markedly larger and more disturbed in the latter case compared with the former, and the latitudinal flow gradients have opposite senses, indicating an expanded flow pattern under southward IMF conditions. For example, at about 1350 UT the vector flows on 29 August 1985 [Fig. 6(d)] increase from 330 m s^{-1} at azimuth 75° in gate 1 to 490 m s^{-1} at azimuth 74° in gate 4, while at the same UT on 27 October 1984 [Fig. 4(g)] they decrease from 1750 m s^{-1} at azimuth 76° in gate 1 to 800 m s^{-1} at azimuth 78° in gate 4.

After about 1400 UT, the IMF once more becomes variable, exhibiting large amplitude 10 min variations in the north–south component (see Fig. 5). In response, the dusk cell flows increase again somewhat, become more uniform across the field-of-view and exhibit ULF wave modulations of moderate (up to about 200 m s^{-1}) amplitude. At no stage, however, do the flows or their modulations reach the peak magnitudes observed on 27 October 1984 [shown, for example, in Fig. 4(g)]. By about 1500 UT (1730 MLT) the flow direction has rotated westward, and the flow modulations have largely died away. At about 1545 UT (1815 MLT) the polar cap boundary region then appears in the highest gates (see Fig. 5), though the flow remains smooth and westward directed at the lowest latitudes sampled until about 1700 UT (1930 MLT). The data shown in Fig. 2 (used to introduce the data format in Section 2) were obtained in the latter region (between 1530 and 1600 UT), and

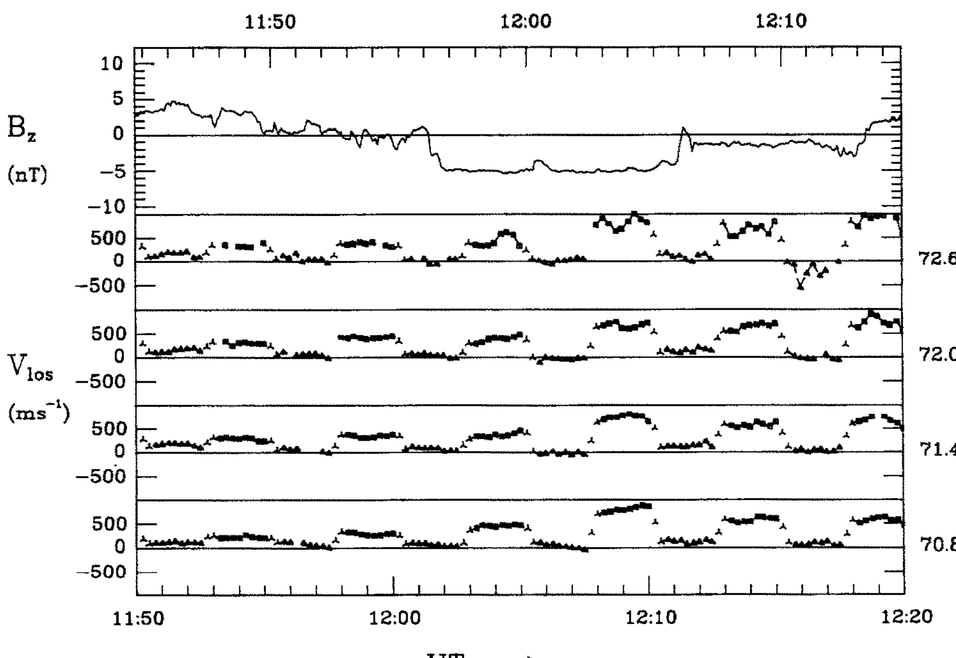

Fig. 6(c). As for Fig. 2, except for the period 1150–1220 UT (1420–1450 MLT) on 29 August 1985. The uncertainties in the l-o-s velocity components are 20, 30, 50 and 85 m s^{-1} for gates 1–4, respectively. In this plot the IMF data have been shifted by 5.3 min relative to the 'Polar' data.

hence correspond to the typically smooth, westward flows of the poleward part of the auroral zone flow cell at dusk. We note again that the polar cap boundary is encountered about 2 h later on this day than on 27 October 1984 due to the different IMF conditions prevailing.

The slow, variable flows of the polar cap boundary region expand rapidly across the field-of-view and first appear in gates 3 and 4 shortly after 1600 UT (1830 MLT), as can be seen on the left hand side of Fig. 6(e). This figure shows 15 s data for the period 1610–1640 UT (1840–1910 MLT), from which it can be seen that little flow is present in the upper gates from about 1613 to 1623 UT. However, at about 1625 UT an increase in westward flow is observed which extends at least to gate 5. It is possible that this increase in flow results from the *northward* turning of the IMF which occurred earlier at about 1604 UT (not shown). When the IMF turns southward again at 1626 UT the flows in gates 3 and 4 return to small values after about 5 min, and, indeed, also very nearly disappear in gate 2 as well. It should be noted that when the radar field-of-view is located in the *poleward* part of the flow cell, a contraction in the cell size resulting from a northward turn of the IMF can cause the flow to increase in magnitude, while an expansion resulting from a southward turn of the field can similarly lead to reduced flows, as is observed in the present case. Thus while we expect, and find, the ionospheric flows to be positively correlated with the southward component of the IMF while the radar field-of-view is located in the equatorward and central portions of the auroral zone flow cells, anti-correlation occurs in the poleward part of the cell, where flow speeds decline with increasing latitude.

After the interval shown in Fig. 6(e), weak and variable flows corresponding to the polar cap boundary region are observed until about 1800 UT (2030 MLT) when, as seen in Fig. 5, equatorward flows of steadily increasing magnitude are detected. In Fig. 6(f) we thus show finally the 15 s data for the interval 1805–1835 UT (2035–2105 MLT) illustrating the growth of this southward flow, which continues to the end of the experiment at 1850 UT (2120 MLT). It can be seen that this flow from the polar cap towards the evening auroral zone is relatively smooth and shows no evidence for ULF wave-like activity, as expected for flow on open flux tubes.

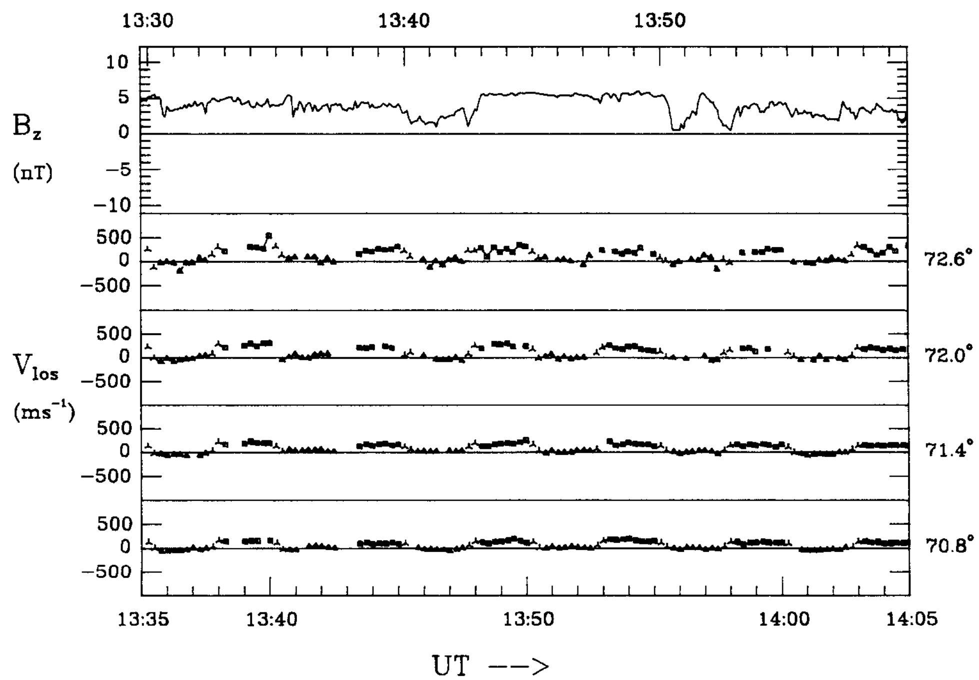

Fig. 6(d). As for Fig. 2, except for the period 1335–1405 UT (1605–1635 MLT) on 29 August 1985. The uncertainties in the l-o-s velocity components are 15, 30, 50 and 80 m s^{-1} for gates 1–4, respectively. In this plot the IMF data have been shifted by 5.3 min relative to the 'Polar' data.

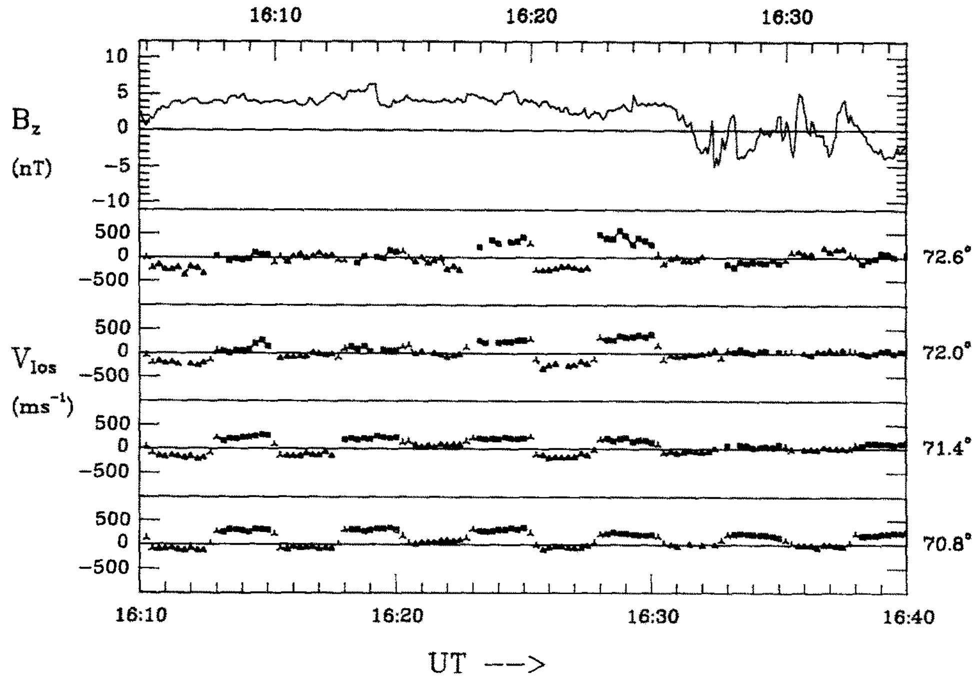

Fig. 6(e). As for Fig. 2, except for the period 1610–1640 UT (1840–1910 MLT) on 29 August 1985. The uncertainties in the l-o-s velocity components are 20, 35, 55 and 80 m s^{-1} for gates 1–4, respectively. In this plot the IMF data have been shifted by 5.3 min relative to the 'Polar' data.

5. SUMMARY

In this paper we have presented a first overview of the high time resolution (15 s) l-o-s velocity components measured at high invariant latitudes (71°–73°) using the EISCAT 'Polar' experiment. Data have been discussed from experiments conducted on two days, 27 October 1984 and 29 August 1985, which, between them, span the local time interval from early morning (about 0200 MLT) to late evening (2130 MLT), and encompass five principal regions of ionospheric flow. With increasing local time these are: (i) the early morning (eastward) auroral zone flow cell; (ii) the dayside region of low flows between and equatorward of the flow cells; (iii) the afternoon and evening (westward) auroral zone flow cell; (iv) the boundary region between the auroral zone and the polar cap; (v) the polar cap region itself. Relatively little data have been examined from the first and last of these regions however, so that our conclusions, to this extent, are somewhat provisional. In Fig. 7 we give a sketch summarizing our results in these five principal regions, where the size and shape of the arrows are intended to indicate the magnitude and character of the flows. The properties of the l-o-s flows observed in these regions are then as follows.

(i) The characteristic feature of the flows in the central region of the dawn auroral zone cell (in the early morning hours) is the irregular variations in the l-o-s components which take place over a range of time scales from about 30 s to 10 min. These fluctuations have amplitudes of the order of a few hundred metres per second, comparable with mean values, such that the data have a characteristically ragged appearance. These observations thus indicate a very irregular flow in this region. The flows are much smoother on the shorter time scales in the equatorward portion of the dawn cell (observed in the immediate pre-dawn hours), though they sometimes exhibit low amplitude undulations with a period of a few minutes.

(ii) In the morning and midday hours, the radar viewing area is located generally between and equatorward of the auroral zone flow cells. L-o-s velocities can remain essentially zero in this region (to within the few tens of metres per second resolution of the data) for extended periods. At other times, sinusoidal ULF pulsations of period about 5 min are present, and can continue for many cycles. The l-o-s amplitude of these waves generally does not exceed about 200 m s^{-1}. 'Beating' between radar beam-swinging and wave cycles can result in spurious, low amplitude, slowly modulated flows being generated in vector maps. The modest flows typical of this region are punctuated on time scales of around 1 or 2 h by bursts of high speed flow, some of which are followed by a damped train of ULF pulsations. These flows have an impulsive onset across the 'Polar' field-of-view, and can reach l-o-s speeds (usually initially poleward) in excess of 1 km s^{-1} after 30 s to 1 min. Further study is required to elucidate the structure and origins of these bursts. One possibility is that they result from impulsive coupling at the Earth's magnetopause, as suggested by TODD *et al.* (1986).

(iii) The equatorward portion of the dusk flow cell (usually encountered in the early afternoon hours), is characterized by modest, smooth flows to the northwest, though continuous waves of periods of a few minutes and about 100 m s^{-1} amplitude are sometimes superposed. In contrast, the faster flows of the central region of the flow cell (generally observed in the mid-afternoon sector), are characterized by their wavy nature. The waves appear to be impulsive in nature, again have periods of a few minutes, and can have large amplitudes, up to many hundreds of metres per second, such that wave and 'background' l-o-s flows have comparable magnitudes. Their possible relationship with the 'flow burst' events merits further investigation. In the late afternoon, the poleward part of the dusk cell comes into the field-of-view. Flow speeds here decrease with increasing latitude and are typically very smooth and featureless.

(iv) A pronounced region of very weak flow has been observed near the dusk meridian between the poleward boundary of westward flows in the dusk cell and the polar cap. The l-o-s components in this region are irregularly directed toward and away from the radar on time scales of minutes, with amplitudes of, at most, 100–200 m s^{-1}. There is no evidence of quasi-sinusoidal ULF wave activity in this region.

(v) Polar cap flows observed in the mid-evening hours are relatively smooth, and again exhibit no evidence for ULF wave activity.

It should be noted that under most of the circumstances discussed above the beam-swinging algorithm used to determine vector flows on time scales of a few minutes should produce meaningful results. The main exceptions to this general conclusion occur in the dayside region of low background flows. When continuous ULF pulsations are present in this region 'beating' between the wave and experiment periods can result in slowly modulated weak flows being deduced. Similarly, the 'flow burst' events and damped wave trains produce spurious large and irregularly directed short-lived flows in vector maps.

In addition to the results above concerning the nature of the high latitude ionospheric flows observed at 15 s resolution, we have also presented considerable further evidence for the close control exerted on these flows by the north–south component of the IMF.

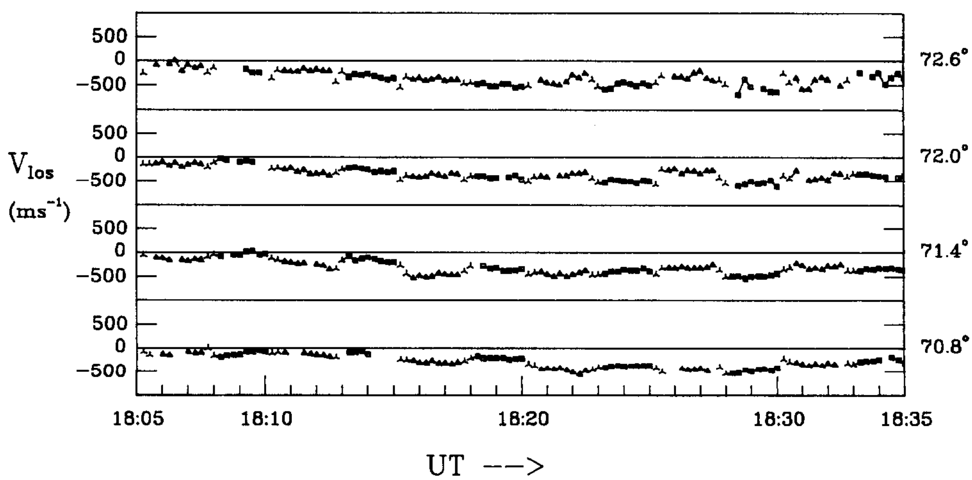

Fig. 6(f). As for Fig. 2, except for the period 1805–1835 UT (2035–2105 MLT) on 29 August 1985. The uncertainties in the l-o-s velocity components are 30, 35, 45 and 60 m s^{-1} for gates 1–4, respectively. No IMF data are available for this interval.

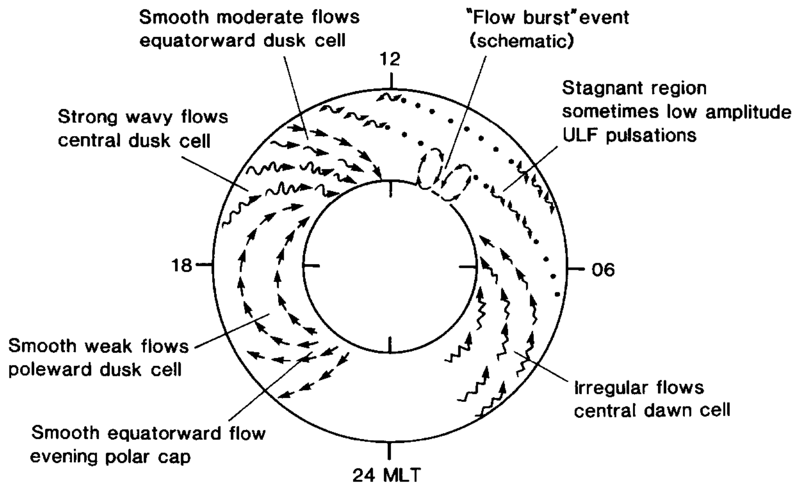

Fig. 7. Sketch summarizing the nature of the high latitude flows observed using the EISCAT 'Polar' experiment from early morning to late evening, in a view looking down on the northern ionosphere (not to scale). The arrows represent the flow vectors and their shape and length are intended to suggest the character of the flows as deduced from the measurements of the l-o-s velocity components at 15 s resolution.

In particular, entry into the dusk cell on both days discussed here was initiated by a southward turning of the IMF, rather than by rotation of the radar viewing area under a fixed pattern. Generally, the variability of the IMF and the rapid response of the dayside flows ensure that the flow variations observed during the dayside hours are temporal rather than spatial in nature. On the first day described here, an abrupt and enduring southward turn in the IMF, which took place when the radar was located in the early afternoon hours, resulted in the excitation of smooth north-westward flows characteristic of the equatorward portion of the dusk flow cell in the radar viewing area, as previously discussed by RISHBETH *et al.* (1985) and LOCKWOOD *et al.* (1986). It should be noted, however, that although the field-of-view was located, presumably, not far equatorward of the pre-existing flow cell at that time, the onset cannot be described in terms of a simple equatorward expansion of that system, since the enhancement was observed simultaneously in all gates. Rather, as described by LOCKWOOD *et al.* (1986), we appear to have observed the temporal excitation of a new twin vortical pattern resulting from reconnection occurring at the magnetopause. On the second day discussed here, entry into the dusk cell occurred in the same MLT sector as in the previous case, but was heralded by the appearance of large impulsive poleward flows and a damped ULF wave train, which was immediately followed by enhanced dusk cell flows. It has been suggested that these impulsive flows resulted from a brief 4 min southward turning of the IMF, the difference in the ionospheric response to the IMF changes on the two days being related to the location of the radar viewing area relative to the footprint of the newly opened flux tubes.

Evidence has also been presented for a rapid response in the magnitude of the westward dusk cell flows observed in the afternoon hours to north–south changes in the IMF. Presumably, changes in both the overall magnitude of the flows as well as the size of the flow pattern are involved here. In the equatorward portion of the flow cell these effects work together to produce a clear positive correlation between the dusk cell flow and southward IMF. In the poleward portion of the cell, however, where flow speeds diminish with increasing latitude (as observed here in the late afternoon and early evening sector), the equatorward expansion of the polar cap during intervals of southward field results in anti-correlation. The latter effect also results in the polar cap boundary being observed in the 'Polar' viewing area at earlier times when the field is southward than when it is northward.

Finally, we wish to emphasize the strong association found here between the central, high speed regions of the auroral zone flow cells and both the large amplitude flow irregularities of the early morning dawn cell and the ULF waves in the afternoon dusk cell. In particular, we anticipate that both the amplitude and the local time of occurrence of ULF waves in the afternoon sector should depend on the north–south component of the IMF. This should lead to correlations between the IMF and ULF waves in the magnetic field at the Earth's surface.

Acknowledgements—We thank the Director and staff of EISCAT for their help, Dr G. Paschmann for the provision of AMPTE IRM plasma data, Professor D. J. Southwood for the provision of AMPTE UKS magnetometer data and Dr W. A. C. Mier-Jedrzejowica for aid in the processing of the latter data. EISCAT is supported by the British SERC, French CNRS, West German MPG, Norwegian NAVF, Swedish NFR and Finnish SA. AMPTE is a collaborative project of NASA (U.S.A.), DFVLR and MPG (F.R.G.) and SERC (U.K.). H.T. was supported by a SERC studentship and A.E. by a SERC grant.

REFERENCES

Alcaydé D., Caudal G. and Fontanari J. 1986 *J. geophys. Res.* **91,** 233.
Allan W. and Poulter E. M. 1984 *Rev. Geophys. Space Phys.* **22,** 85.
Allan W., Poulter E. M., Glassmeier K.-H. and Junginger H. 1985 *Planet. Space Sci.* **33,** 159.
Allan W., White S. P. and Poulter E. M. 1986 *Planet. Space Sci.* **34,** 371.
Clauer C. R. and Banks P. M. 1986 *J. geophys. Res.* **91,** 6959
Clauer C. R., Banks P. M, Smith A. Q., Jorgensen T. S., Friis-Christensen E., Vennerstrom S., Wickwar V. B., Kelly J. D. and Doupnik J. 1984 *Geophys. Res. Lett.* **1,** 9.
Cowley S. W. H. 1984 *Magnetic Reconnection in Space and Laboratory Plasmas*, A.G.U. Geophysical Monograph no. 30, p. 375.
Cowley S. W. H. 1986 *J. Geomagn. Geoelect., Kyoto*, **38,** 1223.
Doupnik J. R., Banks P. M., Baron M. J., Rino C. L. and Petriceks J. 1972 *J. geophys. Res.* **77,** 4268.
Etemadi A., Cowley S. W. H., Lockwood M., Bromage B. J. I., Willis D. M. and Lühr H. 1988 *Planet. Space Sci.* (in press)
Evans J. V., Holt J. M., Oliver W. L. and Wand R. H. 1980 *J. geophys. Res.* **85,** 41.
van Eyken A. P., Rishbeth H., Willis D. M. and Cowley S. W. H. 1984 *J. atmos. terr. Phys.* **46,** 635.
Fairfield D. H. 1971 *J. geophys. Res.* **76,** 6700.
Fontaine D., Perraut S., Alcaydé D., Caudal G. and Higel B. 1986 *J. atmos. terr. Phys.* **48,** 973.
Formisano V. 1979 *Planet. Space Sci.* **27,** 1151.
Formisano V., Domingo V. and Wenzel K.-P. 1979 *Planet. Space Sci.* **27,** 1137.
Foster J. C. 1983 *J. geophys. Res.* **88,** 981.
Foster J. C. and Doupnik J. R. 1984 *J. geophys. Res.* **89,** 9107.
Foster J. C., Doupnik J. R. and Stiles G. S. 1981 *J. geophys. Res.* **86,** 11357.
Foster J. C., Banks P. M. and Doupnik J. R. 1982 *J. geophys. Res.* **87,** 7513.
Goertz C. K., Nielsen E., Korth A., Glassmeier K. H., Haldoupis C., Hoeg P. and Hayward D. 1985 *J. geophys. Res.* **90,** 4069.
Greenwald R. A., Weiss W., Nielsen E. and Thomson N. R. 1978 *Radio Sci.* **13,** 1021.
Jorgensen T. S., Friis-Christensen E., Wickwar V. B., Kelly J. D., Clauer C. R. and Banks P. M. 1984 *Geophys. Res. Lett.* **1,** 887.
Lee L.-C. 1987 *Solar Wind-Magnetosphere Coupling*, p. 297. Terra Scientific Publishing Company.
Lockwood M., van Eyken A. P., Bromage B. J. I., Willis D. M. and Cowley S. W. H. 1986 *Geophys. Res. Lett.* **13,** 72.
Lockwood M., Bromage B. J. I., Horne R. B., St.-Maurice J.-P., Willis D. M. and Cowley S. W. H. 1987 *Geophys. Res. Lett.* **14,** 111.
Lühr H., Klöcker N., Oelschlagel W., Häusler B and Acuña M. 1985 *IEEE Trans. Geosci. Remote Sensing*, **GE-23,** 259.
Nielsen E. 1984 *J. geophys. Res.* **89,** 9095.
Nielsen E., Guttler W., Thomas E. C., Stewart C. P., Jones T. B. and Hedberg A. 1983 *Nature* **304,** 712.
Oliver W. L., Holt J. M., Wand R. H. and Evans J. V. 1983 *J. geophys. Res.* **88,** 5505.
Poulter E. M. and Nielsen E. 1982 *J. geophys. Res.* **87,** 10432.
Poulter E. M., Allan W., Keys J. G. and Nielsen E. 1984 *Planet. Space Sci.* **32,** 1069.

RISHBETH H., SMITH P. R., COWLEY S. W. H., WILLIS D. M., VAN EYKEN A. P., BROMAGE B. J. I. and CROTHERS S. R. 1985 *Nature* **318,** 451.
ROBINSON T. R. 1986 *J. atmos. terr. Phys.* **48,** 417.
SCHLEGEL K., THOMAS E. C. and RIDGE D. 1986 *J. geophys. Res.* **91,** 13,483.
SOFKO G. J., KORTH A. and KREMSER G. 1985 *J. geophys. Res.* **90,** 1449.
SOUTHWOOD D. J. 1985 *Adv. Space Res.* **5,** 4.
SOUTHWOOD D. J. 1987 *J. geophys. Res.* **92,** 3207.
SOUTHWOOD D. J., MIER-JEDRZEJOWICZ W. A. C. and RUSSELL C. T. 1985 *IEEE Trans. Geosci. Remote Sensing* **GE-23,** 301.
TODD H., BROMAGE B. J. I., COWLEY S. W. H., LOCKWOOD M., VAN EYKEN A. P. and WILLIS D. M. 1986 *Geophys. Res. Lett.* **13,** 909.
WICKWAR V. B., KELLY J. D., DE LA BEUJARDIÈRE O., LEGER C. A., STEENSTRUP F. and DAWSON C. H. 1984 *Geophys. Res. Lett.* **1,** 883.
WILLIS D. M., LOCKWOOD M., COWLEY S. W. H., VAN EYKEN A. P., BROMAGE B. J. I., RISHBETH H., SMITH P. R. and CROTHERS S. R. 1986 *J. atmos. terr. Phys.* **48,** 987.